Fractal renewal processes generate $1/f$ noise

S. B. Lowen and M. C. Teich
Columbia Radiation Laboratory, Department of Electrical Engineering, Columbia University, New York, New York 10027
(Received 3 September 1992)

$1/f^D$ noise occurs in an impressive variety of physical systems, and numerous complex theories have been proposed to explain it. We construct two relatively simple renewal processes whose power spectral densities vary as $1/f^D$: (i) a standard renewal point process, with $0 < D < 1$; and (ii) a finite-valued alternating renewal process, with $0 < D < 2$. The resulting event number statistics, coincidence rates, minimal coverings, and autocorrelation functions are shown also to follow power-law forms. These fractal characteristics derive from interevent-time probability density functions which themselves decay in a power-law fashion. A number of applications are considered: trapping in amorphous semiconductors, electronic burst noise, movement in systems with fractal boundaries, the digital generation of $1/f^D$ noise, and ionic currents in cell membranes.

PACS number(s): 05.40.+j, 02.50.−r, 72.80.Ng, 87.10.+e

I. INTRODUCTION

Noise with a power spectral density that varies as an inverse power of frequency is called $1/f^D$ noise [1–5]. $1/f^D$ noise is ubiquitous, occurring in many diverse environments, including resistors and semiconductors [6–8], vacuum tubes [9], traffic [10], and mechanical [11], chemical [12], biological [13], and optical (photon-counting) systems [14]. Mathematical models generating continuous-time $1/f^D$ noise include fractal shot noise [15–17], suitably filtered white Gaussian noise [18], fractionally integrated white noise [19], fractal Brownian motion [20, 21], and a superposition of relaxation processes with an appropriate distribution of time constants [5, 22, 23]. The fractal-shot-noise-driven doubly stochastic Poisson point process is a discrete (point) process that also yields $1/f^D$ noise [24].

In this paper we develop two relatively simple fractal renewal point processes (FRPs) that provide plausible models for a number of physical and biological processes. Both generate $1/f^D$ noise, in the ranges $0 < D < 1$ and $0 < D < 2$, respectively. The first is a standard fractal renewal point process (SFRP), with events represented as points distributed on a line; the second is an alternating fractal renewal process (AFRP), where the process switches between two states (see Fig. 1). Both processes exhibit power-law scaling in many of their statistics, and are therefore fractal. For most of the analysis presented in this paper we consider the case where the processes have reached equilibrium so that the renewal density, or expected rate of events, is constant in time, and thus the processes are stationary. Our FRPs have applications in trapping in amorphous semiconductors, electronic burst noise, movement in systems with fractal boundaries, the digital generation of $1/f^D$ noise, and ionic currents in cell membranes.

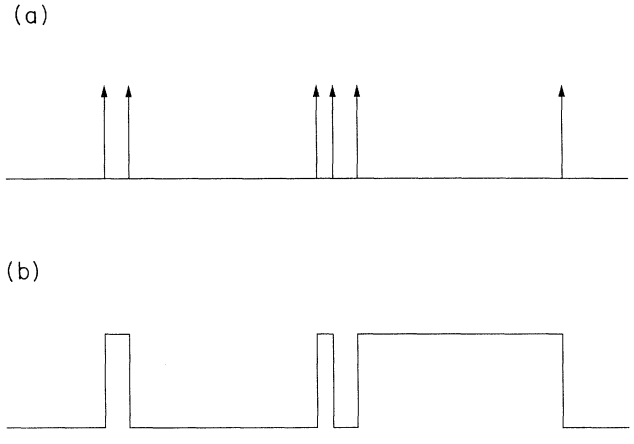

FIG. 1. Sample functions of fractal renewal processes. Interevent times are power-law distributed. (a) The standard fractal renewal process (SFRP) consists of Dirac δ functions and is zero-valued elsewhere. (b) The alternating fractal renewal process (AFRP) switches between values of zero and unity. The symmetric case is shown here.

II. RENEWAL PROCESSES

A standard (nonalternating) renewal process (SRP) $N(t)$ is a point process in which the interevent times are independent random variables drawn from the same probability density, denoted $p(t)$ [see Fig. 1(a)] [25]. We require that $p(t) = 0$ when $t \leq 0$. This density has an associated mean value $\langle T \rangle$, and we define $\mu \equiv \langle T \rangle^{-1}$ to be the average rate of events, where the angle brackets without any subscript $\langle\,\rangle$ represent expectation taken over the distribution of interevent times. We require that the mean interevent time $\langle T \rangle$ be finite, although this requirement may be relaxed in some cases, as in Sec. V C.

Below we summarize a few of the relevant properties of SRPs. The coincidence rate of a stationary (equilibrium) SRP, defined as [26]

$$G_N(\tau) \equiv \lim_{\Delta \to 0} \frac{\Pr\{\mathfrak{E}(t, t+\Delta) \text{ and } \mathfrak{E}(t+\tau, t+\tau+\Delta)\}}{\Delta^2}, \tag{1}$$

where $\mathfrak{E}(x, y)$ represents the occurrence of at least one

event in the interval (x, y), is given by

$$G_N(\tau) = \mu \sum_{n=0}^{\infty} p^{\star n}(|\tau|) = \mu u(t). \tag{2}$$

Here $u(t)$ is the renewal density, and $p^{\star n}(t)$ is $p(t)$ convolved with itself n times (the symbol $\star$ represents the convolution operation). For short delays τ the infinite sum in Eq. (2) may be approximated by its first-order term, yielding $G_N(\tau) \approx \mu p(|\tau|)$, and for long delays the probabilities of events near t and $t+\tau$ are essentially independent, so that $G_N(\tau) \approx \mu^2$.

Treating the events $dN(t)$ in the SRP as Dirac δ functions, the power spectral density becomes [27]

$$S_N(\omega) \equiv \mathcal{F}\{G_N(\tau)\} = \mu^2 \delta(\omega/2\pi) + \mu \mathrm{Re}\left[\frac{1+\phi(\omega)}{1-\phi(\omega)}\right], \tag{3}$$

where $\phi(\,)$ is the characteristic function of the interevent time T. The constant term in the coincidence rate (μ^2) leads to the impulsive (first) term in the power spectral density. In the low-frequency limit the power spectral density approaches an asymptotic value of $\mu^3 \mathrm{Var}\{T\}$ [28], and for high frequencies a value of μ.

For a stationary SRP $N(t)$, the mean rate of events is μ, so that $E\{N(t)\} = \mu t$, where $E\{\,\}$ represents averaging taken over the realizations of the SRP. Using Fourier and Z transforms [28] we obtain expressions for a type of factorial moment

$$E\left\{\frac{[N(t)+k]!}{[N(t)-1]!}\right\} = E\left\{N(t)[N(t)+1]\cdots[N(t)+k]\right\} = \mu(k+1)! \int_0^t (t-v) u^{\star k}(v)\, dv. \tag{4}$$

In particular, the variance is given by

$$\mathrm{Var}\{N(t)\} = 2\mu \int_0^t (t-v)[u(v)-\mu]\, dv - \mu t. \tag{5}$$

An alternating renewal process (ARP) differs from a standard renewal process (SRP) in that the interevent times are drawn alternately from two different distributions, and that the process is generally defined to be finite-valued rather than composed of Dirac δ functions [see Fig. 1(b)]. Consider a process $X(t)$ with two states, valued 0 and 1, respectively. The system alternates between the two states, with the random time T_0 spent in state 0 drawn from the density $p_0(t)$, and the random time T_1 in state 1 drawn from $p_1(t)$. All times are independent of each other. We require that $p_0(t) = p_1(t) = 0$ for $t < 0$, and that the associated mean dwell times $\langle T_0\rangle$ and $\langle T_1\rangle$ be finite, in which case the average value of the process $E\{X\} = \langle T_1\rangle(\langle T_0\rangle + \langle T_1\rangle)^{-1}$ is defined, finite, and positive. The requirement that the mean dwell times be finite may be relaxed in some cases, as in Sec. V C. We note that $X(t)$ can only take values of zero and unity, so that $X^n(t) = X(t)$ for any exponent n, and therefore $E\{X^n\} = E\{X\}$.

The power spectral density for an arbitrary ARP is given by [29]

$$S_X(\omega) = E\{X\}\delta(\omega/2\pi) + \frac{2\omega^{-2}}{\langle T_0\rangle + \langle T_1\rangle} \mathrm{Re}\left\{\frac{[1-\phi_0(\omega)][1-\phi_1(\omega)]}{1-\phi_0(\omega)\phi_1(\omega)}\right\}, \tag{6}$$

where $\phi_0(\,)$ and $\phi_1(\,)$ are the characteristic functions of the dwell times T_0 and T_1, respectively. For a Markovian system, where both dwell times are exponentially distributed, the power spectral density assumes the familiar Lorentzian form

$$S_X(\omega) = E\{X\}\delta(\omega/2\pi) + \frac{k}{(\omega/\omega_0)^2 + 1}, \tag{7}$$

where $\omega_0 \equiv \langle T_0\rangle^{-1} + \langle T_1\rangle^{-1}$ and $k \equiv 2\omega_0^{-2}(\langle T_0\rangle + \langle T_1\rangle)^{-1}$. Returning to the general ARP, in the low-frequency limit the power spectral density approaches an asymptotic value [28]

$$\lim_{\omega\to 0} S_X(\omega) = \frac{\langle T_0\rangle^2 \mathrm{Var}\{T_1\} + \langle T_1\rangle^2 \mathrm{Var}\{T_0\}}{(\langle T_0\rangle + \langle T_1\rangle)^3}, \tag{8}$$

whereas for $\omega \to \infty$,

$$S_X(\omega) \to 2\omega^{-2}(\langle T_0\rangle + \langle T_1\rangle)^{-1}. \tag{9}$$

In the special case $p_0(t) = p_1(t) = p(t)$, with arbitrary $p(t)$, the power spectral density simplifies to [30]

$$S_X(\omega) = \tfrac{1}{2}\delta(\omega/2\pi) + \mu\omega^{-2}\mathrm{Re}\left\{\frac{1-\phi(\omega)}{1+\phi(\omega)}\right\}. \tag{10}$$

In this case the autocorrelation function is given by [28]

$$R_X(\tau) = \frac{1}{2} - \frac{1}{2}\sum_{n=0}^{\infty}(-1)^n \int_0^t r \star p^{\star n}(v)\, dv, \tag{11}$$

where

$$r(t) \equiv \mu \int_t^{\infty} p(v)\, dv \tag{12}$$

is the recurrence time density. For small delays τ, the probability of a state transition occurring in the interval $(t, t+\tau)$ is nearly zero, so that $R_X(\tau) \approx E\{X^2\} = \frac{1}{2}$, while for large delays τ, the states of X at t and $t+\tau$ are essentially independent, so that $R_X(\tau) \approx E\{X\}^2 = \frac{1}{4}$.

For the case where the times T_1 spent in state 1 are much smaller than the times T_0 spent in state 0, the power spectral density reduces to a simpler form related to the result for the SRP [28]

$$S_X(\omega) \approx \frac{\langle T_1\rangle}{\langle T_0\rangle}\delta(\omega/2\pi) + \frac{2\langle T_1\rangle^2}{\langle T_0\rangle}\mathrm{Re}\left\{\frac{\phi_0(\omega)}{1-\phi_0(\omega)}\right\}. \tag{13}$$

Geometrically, the ARP $X(t)$ itself looks like a SRP if the time spent in state 1 is small; $X(t)$ remains in state 0 except for relatively brief visits to state 1. In this case the process may be modeled as a marked SRP, where the marking values correspond to the widths of the pulses, which are independent and identically distributed according to $p_1(t)$. This approximation holds for time scales

greater than the characteristic time of T_1; for times less than this the Lorentzian approximation of Eq. (7) holds.

III. FRACTAL RANDOM VARIABLES

Fractals are distinguished by power-law scaling behavior; we consider fractal random variables that have a power-law decay in their associated probability density functions. Fractal renewal processes may be constructed from these random variables. Such power-law behavior cannot persist for all values of the random variable since the resulting probability density would not be able to be normalized. We consider the general case with cutoffs in the probability density at both extremely large and extremely small values, which ensures that the FRPs will have a positive rate in the stationary state (equilibrium) (see Fig. 2).

Possibly the simplest such interevent-time density is the abrupt-cutoff power-law density

$$p(t) = \frac{D}{A^{-D} - B^{-D}} \times \begin{cases} t^{-(D+1)} & \text{for } A < t < B, \\ 0 & \text{otherwise.} \end{cases} \tag{14}$$

The associated moments are given by

$$\langle T^n \rangle = \frac{D}{n-D}(A/B)^D B^n \frac{1-(A/B)^{n-D}}{1-(A/B)^D}, \tag{15}$$

and the characteristic function of the interevent time is

$$\phi(\omega) = \frac{D(-j\omega)^D}{A^{-D} - B^{-D}} \int_{-j\omega A}^{-j\omega B} e^{-x} x^{-(D+1)}\, dx. \tag{16}$$

In the case $B^{-1} \ll \omega \ll A^{-1}$, then [28]

$$1 - \phi(\omega) \approx (-j\omega A)^D \Gamma(1-D). \tag{17}$$

Another density with essentially the same power-law dependence but with smoother transitions is

$$p(t) = \frac{(AB)^{D/2}}{2K_D(2\sqrt{A}/\sqrt{B})} e^{-A/t} e^{-t/B} t^{-(D+1)}, \tag{18}$$

where $K_D(\,)$ is the modified Bessel function of the second kind of order D. The associated moments are given by

$$\langle T^n \rangle = (AB)^{n/2} \frac{K_{|D-n|}(2\sqrt{A}/\sqrt{B})}{K_D(2\sqrt{A}/\sqrt{B})}, \tag{19}$$

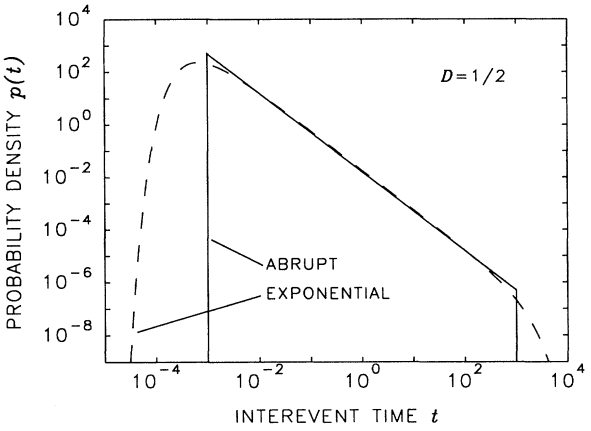

FIG. 2. Double logarithmic plot of two fractal interevent-time probability density functions $p(t)$ vs t for $D = \frac{1}{2}$: abrupt-cutoff and exponential-cutoff power-law ($A = 10^{-3}$, $B = 10^3$). Note the power-law region between $t = A$ and $t = B$.

with corresponding characteristic function

$$\phi(\omega) = (1 - j\omega B)^{D/2} \frac{K_D(2(A/B - j\omega A)^{1/2})}{K_D(2\sqrt{A}/\sqrt{B})}. \tag{20}$$

For $D = \frac{1}{2}$ and $B \to \infty$ this density becomes the one-sided Lévy-stable density of order $\frac{1}{2}$ [31]. Combined with exponential tails, one-sided Lévy-stable densities for arbitrary D between zero and unity also follow a power-law form while providing smooth transitions [28].

IV. FRACTAL RENEWAL PROCESSES

The fractal probability densities defined in Sec. III may be used to construct well-defined SRPs, since the densities are zero for nonpositive arguments.

For the abrupt-cutoff power-law process the power spectral density exhibits $1/f^D$ behavior, but contains significant oscillations arising from the abrupt nature of the interevent-time density. In the medium-frequency limit, $B^{-1} \ll \omega \ll A^{-1}$, we obtain [28]

$$S_N(\omega) \to \mu \times \begin{cases} 2[\Gamma(1-D)]^{-1} \cos(\pi D/2)(\omega A)^{-D} & \text{for } 0 < D < 1, \\ \pi[\ln(\omega A)]^{-2}(\omega A)^{-1} & \text{for } D = 1, \\ 2D^{-2}(D-1)\Gamma(2-D)[-\cos(\pi D/2)](\omega A)^{D-2} & \text{for } 1 < D < 2, \\ \frac{1}{2}[-\ln(\omega A)] & \text{for } D = 2, \\ D^{-1}(D-2)^{-1}(D-1)^2 & \text{for } D > 2. \end{cases} \tag{21}$$

Figure 3 shows the resulting power spectral density, normalized to unity at the low-frequency limit, where the asymptotes are given by Eq. (21) and Sec. II. The abrupt cutoff in the probability density function leads to large oscillations in the characteristic function, which appear in the power spectral density. Thus for $0 < D < 1$ the power spectral density varies as $1/f^D$ over a substantial range of frequencies $B^{-1} \ll \omega = 2\pi f \ll A^{-1}$, which may be made as large as desired, where D corresponds to the power-law exponent in the interevent-time density. However, this power-law exponent never reaches unity, and no new exponents are introduced by consider-

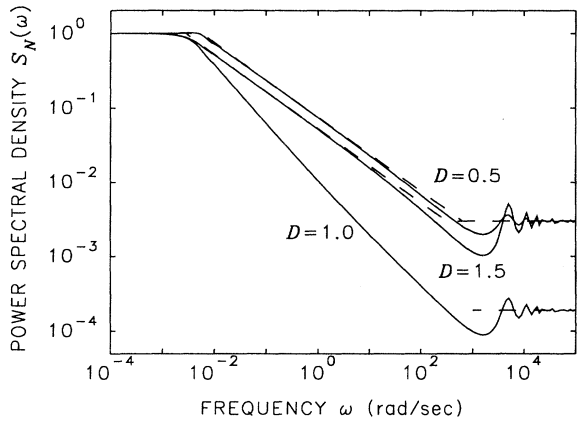

FIG. 3. Double logarithmic plot of the normalized power spectral density for the SFRP, with an abrupt-cutoff power-law probability density. Three values of the exponent D are shown: 0.5, 1.0, and 1.5 ($A = 10^{-3}$, $B = 10^3$). Asymptotic forms from Eq. (21) and Sec. II are included for comparison. The abrupt cutoff in the interevent-time probability density function gives rise to oscillations in the frequency domain, especially for larger values of D.

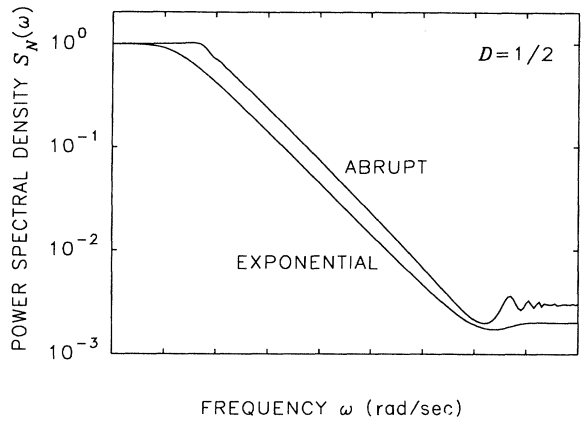

FIG. 4. Double logarithmic plot of the normalized power spectral density for the SFRP, comparing abrupt-cutoff and exponential-cutoff power-law probability densities ($D = \frac{1}{2}$, $A = 10^{-3}$, $B = 10^3$). The exponential-cutoff density has smoother transitions in the time domain, which lead to less oscillation in the frequency domain.

ing $D > 1$. Presumably any probability density having a power-law form would show the same behavior, and thus the SFRP will generate $1/f^D$ noise only in the range $0 < D < 1$. Figure 4 shows the power spectral density for the abrupt- and exponential-cutoff densities with $D = \frac{1}{2}$. The exponential-cutoff density has a relatively smooth shape, and thus the resulting power spectral density exhibits less oscillation. The essential power-law character of the power spectral density, however, is unchanged.

An approximation for the coincidence rate of the abrupt-cutoff power-law process may be obtained by inverse Fourier transforming the quantity given in Eq. (21), which for $0 < D < 1$ yields

$$G_N(\tau) \approx (\pi D)^{-1} B^{D-1} A^{-2D} \sin(\pi D) |\tau|^{D-1} \tag{22}$$

in the range $A \ll |\tau| \ll B$.

For the interevent-time density given in Eq. (18) and the particular case $D = \frac{1}{2}$, useful expressions may be obtained for the coincidence rate, and Eq. (2) yields

$$\begin{aligned} G_N(\tau) &= \mu\delta(\tau) + \mu \sum_{n=1}^{\infty} p^{*n}(|\tau|) \\ &= (AB)^{-1/2}\delta(\tau) + (\pi B)^{-1/2}|\tau|^{-3/2} e^{-|\tau|/B} \\ &\quad \times \sum_{n=1}^{\infty} n \exp\left[2(A/B)^{1/2} n - (A/|\tau|)n^2\right]. \end{aligned} \tag{23}$$

In the limit $|\tau| \gg A$ and $B \gg A$, the terms in the sum vary slowly, so the sum may be approximated by an integral, and the coincidence rate simplifies to

$$\begin{aligned} G_N(\tau) &\approx (\pi B)^{-1/2}|\tau|^{-3/2} e^{-|\tau|/B} \int_0^{\infty} x \exp\left[2(A/B)^{1/2} x - (A/|\tau|)x^2\right] dx \\ &= (4\pi A^2 B)^{-1/2} |\tau|^{-1/2} e^{-|\tau|/B} + (2AB)^{-1} \operatorname{erfc}(-|\tau|^{1/2} B^{-1/2}), \end{aligned} \tag{24}$$

where

$$\operatorname{erfc}(x) \equiv 2\pi^{-1/2} \int_x^{\infty} \exp(-t^2)\, dt \tag{25}$$

is the complementary error function. Figure 5 shows the coincidence rate for $D = \frac{1}{2}$ as provided by Eqs. (23) and (24).

For the case $A \ll |\tau| \ll B$ and $0 < D < 1$, but with arbitrary cutoffs, we have $u(t) \sim t^{D-1}$, so that $u^{*k}(t) \sim t^{kD-1}$, and Eq. (4) provides

$$E\left\{\frac{[N(t)+k]!}{[N(t)-1]!}\right\} \sim t^{kD+1}. \tag{26}$$

The constants of proportionality depend on the details of the interevent-time probability density function. In particular, for the abrupt-cutoff SFRP, $E\{N(t)\} = \mu t$ and substituting Eq. (22) into Eq. (5) yields

$$\operatorname{Var}\{N(t)\} \approx \left[\pi D^2 (D+1)\right]^{-1} B^{D-1} A^{-2D} \sin(\pi D) t^{D+1}. \tag{27}$$

Calculation of the capacity dimension yields the expected result that, for the parameter ranges $0 < D < 1$ and $0 < A \ll B < \infty$, the set of points generated by the SFRP is itself fractal with dimension D. Consider a realization of the process, and a covering of it using segments of length L. For a minimal covering, place the beginning of each segment on the first uncovered event, in which

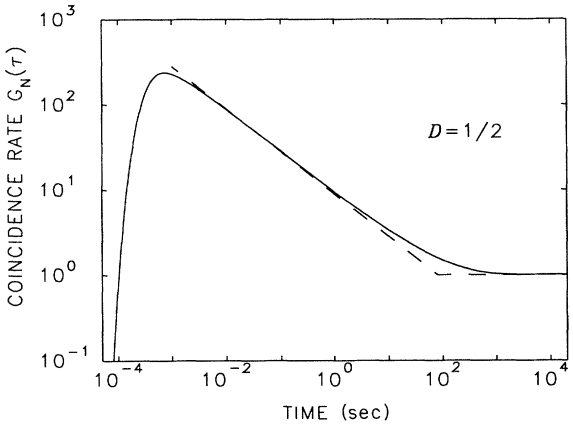

FIG. 5. Double logarithmic plot of the coincidence rate for the SFRP, with the exponential-cutoff probability density function, for $D = \frac{1}{2}$ ($A = 10^{-3}$, $B = 10^3$). Asymptotes are provided in Sec. II, and by simplification of Eq. (24) in the limit $|\tau| \ll B$.

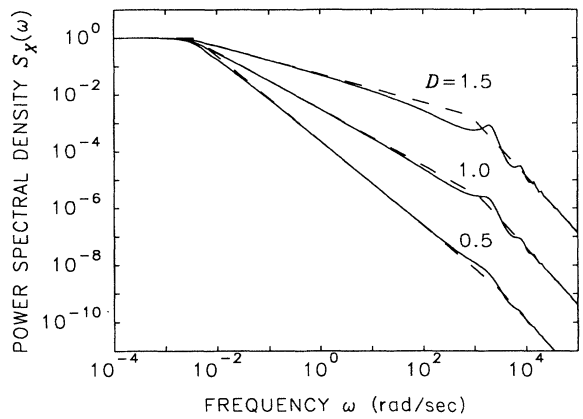

FIG. 6. Double logarithmic plot of the normalized power spectral density for the AFRP, with an abrupt-cutoff power-law probability density. Three values of the exponent D are shown: 0.5, 1.0, and 1.5 ($A = 10^{-3}$, $B = 10^3$). Asymptotic forms from Eqs. (8), (9), and (29) are included for comparison. The abrupt cutoff in the interevent-time probability density function gives rise to oscillations in the frequency domain, especially for larger values of D.

case the empty space between coverings is simply the residual waiting time for a pure renewal process at time L. If $W(L)$ represents the expected value of the time between coverings, including the coverings themselves, then by Wald's lemma [31]

$$W(L) = \langle T \rangle \int_0^L u(t)\, dt. \tag{28}$$

For the range $A \ll L \ll B$, the approximation $u(t) \sim t^{D-1}$ provides $W(L) \sim L^D$. Thus the number of intervals required to cover the SFRP will scale as L^{-D}, and the capacity dimension is D.

The AFRP by construction resembles the SFRP, so many of the characteristics derived above apply to the AFRP as well. The symmetric AFRP and the SFRP by definition have identical transition number statistics; the only difference is that the AFRP transitions are of two types which alternate. For the extreme asymmetric AFRP, where T_1 is very short compared to T_0, a different correspondence exists. Here the state transitions occur in closely spaced pairs of negligible width, and thus the AFRP transition-*pair* number statistics are essentially identical to the SFRP single transition number statistics. In addition, in the extreme asymmetric case the AFRP power spectral density (and thus the coincidence rate) are proportional to the SFRP results except for the high-frequency (short-time) limit, in which case the AFRP power spectral density varies as $S_X(\omega) \approx 2\omega^{-2}/\langle T_0 \rangle$.

For dwell times of the two states given by identical, abrupt-cutoff power-law distributions, the power spectral density also varies as $1/f^D$, but with a different form from that of the SFRP. In the medium-frequency limit ($A^{-1} \ll \omega \ll B^{-1}$) we obtain [28]

$$S_X(\omega) \to \frac{\mu}{4} \times \begin{cases} 2\Gamma(1-D)\cos(\pi D/2) A^D \omega^{D-2} & \text{for } 0 < D < 1, \\ \pi A \omega^{-1} & \text{for } D = 1, \\ 2(D-1)^{-1}\Gamma(2-D)\left[-\cos(\pi D/2)\right] A^D \omega^{D-2} & \text{for } 1 < D < 2, \\ 2A^2\left[-\ln(\omega A)\right] & \text{for } D = 2, \\ D(D-2)^{-1} A^2 & \text{for } D > 2, \end{cases} \tag{29}$$

for the abrupt-cutoff power-law interevent-time density. Figure 6 shows the resulting power spectral density, normalized to unity at the low-frequency limit, where the asymptotes are given by Eqs. (8), (9), and (29). Note that the power spectral density has an overall $1/f^D$ shape. Thus the AFRP generates $1/f^D$ noise in the full range $0 < D < 2$ over a substantial range of frequencies $B^{-1} \ll \omega = 2\pi f \ll A^{-1}$, which may be made as large as desired.

The autocorrelation function, like the coincidence rate, will show power-law behavior in some cases, since it is the inverse Fourier transform of the power-law-varying power spectral density. For D between 1 and 2, then Eq. (29) yields

$$R_X(\tau) - E\{X\}^2 \approx (2D)^{-1}\left[-\cos(\pi D/2)\right] A^{D-1} |\tau|^{1-D} \tag{30}$$

for $A \ll |\tau| \ll B$. When $0 < D \leq 1$, then the autocorrelation function assumes a constant value in the limit $A \ll |\tau| \ll B$ [28].

V. GENERALIZATIONS OF FRACTAL RENEWAL PROCESSES

A. Filtering

The events in the SFRP may be treated as Dirac δ functions (impulses) distributed along the time axis, so

a natural extension to the above theory is to pass these impulses through a linear filter. This results in a kind of generalized shot noise [27]. For a deterministic filter, the resulting overall power spectral density is given by linear systems theory [25]

$$S(\omega) = |H(\omega)|^2 S_N(\omega) = \mu |H(\omega)|^2 \mathrm{Re}\left\{\frac{1+\phi(\omega)}{1-\phi(\omega)}\right\}, \tag{31}$$

where $H(\omega)$ is the Fourier transform of the linear-system impulse response function $h(t)$. The AFRP may also be filtered.

For the AFRP with $\Pr\{T_1 > T_0\} \ll 1$, the resulting process may be modeled as a marked SFRP, as in Sec. IV, or as a randomly filtered SFRP. In this case the impulse response function of the filter will have a rectangular shape with fixed height and random duration given by the density $p_1(t)$.

The power spectral density in Eq. (3), without filtering, approaches an asymptote of μ for large frequencies ω, and therefore the total power integral $\int_{-\infty}^{\infty} S_N(\omega)\, d\omega/2\pi$ is unbounded. Real systems, however, have a frequency response which decreases faster than ω^{-1} for sufficiently large ω, yielding finite energy integrals.

B. Superposition of renewal processes

A different point process will result when several SFRPs are superposed, but the overall power spectral density will still be $1/f^D$. Consider M identical and independent SFRPs. We define the conditional coincidence rate as

$$G_{N,nm}(\tau) \equiv \lim_{\Delta\to 0} \frac{\Pr\{\mathfrak{E}_n(t,t+\Delta) \text{ and } \mathfrak{E}_m(t+\tau,t+\tau+\Delta)\}}{\Delta^2}, \tag{32}$$

where $\mathfrak{E}_n(x,y)$ represents the occurrence of an event in the interval (x,y) due to the individual SFRP indexed by n, where $1 \le n \le M$. For the same SFRP ($n = m$), the conditional coincidence rate is the same as that given in Eq. (2), while for $n \ne m$, the two processes are independent, and we have $G_{N,n\neq m} = \mu^2$. Therefore the total coincidence rate $G_{N,T}(\tau)$, due to all M individual SFRPs, is given by

$$\begin{aligned} G_{N,T}(\tau) &= \sum_n \sum_m G_{N,nm}(\tau) = \sum_n \sum_{m(\neq n)} G_{N,nm}(\tau) + \sum_n G_{N,nn}(\tau) \\ &= \sum_n \sum_{m(\neq n)} \mu^2 + \sum_n G_N(\tau) = (M^2 - M)\mu^2 + M G_N(\tau) \\ &= (M^2 - M)\mu^2 + M\mu \sum_{i=0}^{\infty} p^{\star n}(|\tau|). \end{aligned} \tag{33}$$

As the number M of independent SFRPs increases, the impulsive term grows as $M^2 - M$ while the smooth term increases only as M; thus for large M the impulsive term dominates, as it would for most point processes with high rates. The corresponding power spectral density is

$$\begin{aligned} S_{N,T}(\omega) &= (M^2 - M)\mu^2 \delta(\omega/2\pi) + M S_N(\omega) \\ &= (M\mu)^2 \delta(\omega/2\pi) + (M\mu)\mathrm{Re}\left\{\frac{1+\phi(\omega)}{1-\phi(\omega)}\right\}. \end{aligned} \tag{34}$$

Thus for $\omega \ne 0$ the shape of the power spectral density is independent of M. Indeed, Eq. (34) shows that to second order, the superposition of M SFRPs with identical rates μ is exactly equivalent to a single SFRP with rate $M\mu$. Thus the superposition process tends to a clustered Poisson process limit [32]. The number of events in small intervals ($t \ll A$) will be independent Poisson-distributed random variables, but for longer times ($A \ll t \ll B$), the process will exhibit clustering, described by the coincidence rate $G_{N,T}(\tau)$ given in Eq. (33) above. In particular, for $B^{-1} \ll |\omega| \ll A^{-1}$ the $1/f^D$ character is preserved. For applications where this frequency range is important, the impulsive term in the power spectral density may be removed with a high-pass filter.

An identical argument for the AFRP yields the same results. Here the total autocorrelation $R_{X,T}(\tau)$, due to all M individual AFRPs, is given by

$$R_{X,T}(\tau) = (M^2 - M)E\{X\}^2 + M R_X(\tau), \tag{35}$$

and the corresponding power spectral density is

$$S_{X,T}(\omega) = (M^2 - M)E\{X\}^2 \delta(\omega/2\pi) + M S_X(\omega). \tag{36}$$

Since $E\{X^n\} = E\{X\} = \langle T_1\rangle(\langle T_0\rangle + \langle T_1\rangle)^{-1} < \infty$ in general, then the first and second moments of the AFRP $X(t)$ are finite in particular, and the total process $X_T(t)$ will converge to a Gaussian process with mean $ME\{X\}$, and autocovariance function $M[R_X(\tau) - E\{X\}^2]$.

C. Nondegenerate realization of a zero-rate process

For stationary (equilibrium) SFRPs constructed from infinite-tail power-law distributions with $D \le 1$, the mean interevent time is infinite, and thus the mean rate of events is zero. Since the rate is non-negative, this implies with probability one that no events will be observed in any finite interval. However, the framework developed above for the stationary SFRP may be extended to yield nontrivial results in this case. (All the results in this

section also apply for symmetric AFRPs.) For SRPs beginning with an event, rather than in equilibrium, the above does not apply, and the resulting *energy* spectral density will not be degenerate. A segment of such a SRP may therefore contain a positive number of events, even though the mean number of events in the segment of the stationary process is zero. For both of the fractal random variables considered in this paper, if the outer cutoff B is set to infinity, then the probability of observing no events in a segment of length C can still be made vanishingly small as the ratio C/A increases, where A is the inner cutoff. A SFRP beginning at an event, with an associated interevent-time probability density function $p(t) \sim t^{-(1+D)}$, will have a residual waiting time that approaches a limiting density [31]. Specifically, suppose that the interevent-time survivor distribution may be put in the form

$$1 - P(t) = \int_t^\infty p(v)\,dv = t^{-D}L(t), \tag{37}$$

where $L(t)$ is a "slowly varying" function such that

$$\lim_{t\to\infty} L(xt)/L(t) = 1 \tag{38}$$

for any $x > 0$. Now define $Z(t)$ to be the random variable denoting the time between the deterministic time t and the next event in the SFRP. Then $Z(t)$ has the density [31]

$$p_Z(z) = \frac{t^D \sin(\pi D)}{\pi} \frac{z^{-D}}{z+t}. \tag{39}$$

Thus when a SFRP with zero mean rate begins on an event, the resulting process has a nonzero effective rate for all finite times. Therefore, any experiment will of necessity measure a process with positive expected rate, and the results derived above will also apply to this process.

For any realization of an infinite-mean SFRP which begins with an event, and which is observed for a finite time, there will be a largest and a smallest interval, labeled T_B and T_A, respectively. Given the power-law exponent of the distribution and only the values of T_A and T_B, the other intervals will be power-law distributed between them, also with the same power-law exponent. Thus the observed process will have the same statistics as a finite-mean SFRP with cutoff times $A < T_A$ and $B > T_B$, and the results derived above apply to this process, with the *a posteriori* values of T_A and T_B. Although these values T_A and T_B cannot be known *a priori*, the sample power spectrum will decay in a power-law fashion whatever these values may be.

VI. APPLICATIONS

A. Trapping in amorphous semiconductors

The multiple trapping model as developed by Orenstein and Kastner [33,34], and Tiedje and Rose [35] shows how exponentially distributed traps over a large range of energies lead to a power-law decay of current in an amorphous semiconductor. If a pulse of light strikes such a semiconductor, then many carriers will be excited out of their traps and are available to carry current until they are recaptured by a trap, which happens relatively quickly. At some point each carrier will be released from its trap by thermal excitation and become mobile for a time, and then be recaptured by another trap. For exponentially distributed states with identical capture cross sections, the electrons will tend to be trapped in shallow states at first, but the probability of being in a deep trap will increase as time progresses. This leads to a current which decreases as a power-law function of time.

In this section we recast the multiple trapping model in terms of the SFRP [36, 28]. Consider an amorphous semiconductor with localized states (traps) which are exponentially distributed with parameter $\mathcal{E}_0$ between limits of $\mathcal{E}_L$ and $\mathcal{E}_H$. If the random variable $\mathcal{E}$ represents the energy difference between a trap and the conduction band edge, then the probability density function for the states $p_\mathcal{E}(\mathcal{E})$ is given by

$$p_\mathcal{E}(\mathcal{E}) = \begin{cases} k\exp(-\mathcal{E}/\mathcal{E}_0) & \text{for } \mathcal{E}_L < \mathcal{E} < \mathcal{E}_H, \\ 0 & \text{otherwise,} \end{cases} \tag{40}$$

where

$$k \equiv \mathcal{E}_0^{-1}\left[\exp(-\mathcal{E}_L/\mathcal{E}_0) - \exp(-\mathcal{E}_H/\mathcal{E}_0)\right]^{-1} \tag{41}$$

is a normalizing constant. Since band gaps always have finite widths, every semiconductor will have a maximum trap depth, and thus $\mathcal{E}_H$ will be finite. Similarly, $\mathcal{E}_L$ must be greater than zero. Very shallow traps, with energies $\mathcal{E} \ll k_B\mathcal{T}$, where k_B is Boltzmann's constant and $\mathcal{T}$ is the absolute temperature, will be occupied so infrequently that they can be neglected. There may be other practical limits which impose a larger $\mathcal{E}_L$.

For a trap with energy $\mathcal{E}$, the corresponding mean waiting time τ is $\tau_0\exp(\mathcal{E}/k_B\mathcal{T})$, where τ_0 is the average vibrational period of the atoms in the semiconductor. If we define characteristic time cutoffs $A \equiv \tau_0\exp(\mathcal{E}_L/k_B\mathcal{T})$ and $B \equiv \tau_0\exp(\mathcal{E}_H/k_B\mathcal{T})$, and the power-law exponent $D \equiv k_B\mathcal{T}/\mathcal{E}_0$, then the mean waiting time τ has the power-law density

$$p(t) = \frac{D}{A^{-D} - B^{-D}} \times \begin{cases} t^{-(D+1)} & \text{for } A < t < B, \\ 0 & \text{otherwise.} \end{cases} \tag{42}$$

Each trap holds carriers for times that are exponentially distributed, given the conditional parameter τ

$$p_T(t|\tau) = \tau^{-1}e^{-t/\tau}. \tag{43}$$

Averaging this exponential density over all possible values of τ yields the unconditional trapping-time density

$$\begin{aligned} p(t) &= \int_\tau p_T(t|\tau)p_\tau(\tau)\,d\tau \\ &= \frac{D}{A^{-D} - B^{-D}} t^{-(D+1)} \int_{t/B}^{t/A} x^D e^{-x}\,dx. \end{aligned} \tag{44}$$

For $A \ll B$, which is usually the case, the unconditional trapping time density has the asymptotic forms

$$p(t) \approx \begin{cases} D(D+1)^{-1}A^{-1} & \text{for } t \ll A, \\ D\Gamma(D+1)A^D t^{-(D+1)} & \text{for } A \ll t \ll B, \\ D(A/B)^D t^{-1} e^{-t/B} & \text{for } t \gg B. \end{cases} \quad (45)$$

Thus each carrier will be trapped for a period which is essentially power-law distributed.

Upon escaping from a trap, the carrier can conduct current for a relatively short time until it is again captured by another trap. Thus each carrier executes a series of current-carrying jumps well described by the AFRP with extreme asymmetry, which is in turn well approximated by a marked SFRP. If the experiment begins with a pulse of light then the SFRP begins on an event; if the experiment begins after transients have died out then the SFRP is in equilibrium. Assuming that each carrier acts independently of the others, then the action of the carriers as a whole can be modeled as the superposition of SFRPs. In particular, the steady-state current should behave as impulsive $1/f^D$ noise. Indeed, experimental [37] and theoretical [38] results show exactly this type of frequency dependence, with $0 < D < 1$.

As a check we consider the resistivity as a function of temperature, which to first order follows the form [39]

$$\rho(\mathcal{T}) = \rho_0 \exp(\mathcal{E}_\rho / k_B \mathcal{T}). \quad (46)$$

Since the time the carriers spend outside the traps is relatively small, the resistivity should vary directly with the average time spent in the traps, which is

$$\langle \tau \rangle_\tau \approx \frac{D}{1-D} B^{1-D} A^D \quad (47)$$

for $B \gg A$ and $0 < D < 1$. Substituting for A, B, and D as defined above in this section we obtain

$$\langle \tau \rangle_\tau = \tau_0 (\mathcal{E}_0 / k_B \mathcal{T} - 1)^{-1} \exp[-(\mathcal{E}_H - \mathcal{E}_L)/\mathcal{E}_0] \times \exp(-\mathcal{E}_H / k_B \mathcal{T}), \quad (48)$$

so that

$$\rho(\mathcal{T}) \sim (\mathcal{E}_0 / k_B \mathcal{T} - 1)^{-1} \exp(-\mathcal{E}_H / k_B \mathcal{T}). \quad (49)$$

For an exponential distribution of trap energies with a long tail, $\mathcal{E}_H \gg \mathcal{E}_0$; since $\mathcal{E}_0 > k_B \mathcal{T}$, then to first order

$$\rho(\mathcal{T}) \approx \rho_0 \exp(-\mathcal{E}_H / k_B \mathcal{T}). \quad (50)$$

Finally, a simpler model, which invokes power-law distributed trapping times directly, also generates $1/f^D$ noise [40]. In particular, trapping times distributed as τ^{-2} generate both current and resistance fluctuations which vary as $1/f^1$.

B. Electronic burst noise

Burst noise occurs in many communications systems and is characterized by relatively brief noise events which cluster together, separated by relatively longer periods of quiet. Mandelbrot [41] showed that burst errors in communication systems are well modeled by a version of the SFRP, and in particular that the interevent times were essentially independent of each other. In his model the upper cutoff B was infinite, and the lower cutoff A was defined by the resolution of the observation. However, the interevent-time histograms shown do not follow a power-law form for very large values of the interevent time, but rather decrease in a fashion consistent with an exponential tail. Thus the exponential-cutoff density described above should apply to burst noise in electronic systems. In addition, some systems may contain several independent sources of burst noise, and therefore the superposition of several SFRPs should model these noise sources.

C. Movement in systems with fractal boundaries

If a particle moves in a system with two simple basins of attraction and a white-noise forcing function, then the dwell times in the basins will be independent and exponentially distributed, leading to the familiar Lorentzian spectrum. However, if the boundary between the two attractors is fractal, then the distance between the particle and the boundary will be distributed over a large range of scale lengths, leading to power-law distributed or fractal dwell times [42]. Similarly, one-dimensional deterministic mappings such as the modified Bernoulli system can lead to fractal dwell times [43, 30]. In both cases the two states of the system are symmetric, and thus the system is well modeled by the AFRP.

D. Digital generation of $1/f^D$ noise

In addition to being a useful description of unavoidable $1/f^D$ noise, the FRP model may be used for deliberately generating test signals with power spectral densities varying as $1/f^D$. Indeed, the particular case $D = 1$, which corresponds to precisely $1/f$ noise, has equal power per octave and is useful in audio testing. If U is a random variable uniformly distributed in the interval $0 < U < 1$, then the transformed random variable

$$T \equiv A\left\{[1 - (A/B)^D]U + (A/B)^D\right\}^{-1/D} \quad (51)$$

has the power-law density of Eq. (14). Thus a conventional computer random number generator may be used to generate a real approximation to the AFRP model which varies as $1/f^D$ for any D in the range $0 < D < 2$. For practical implementation, the random variable T may be approximated as a multiple N of some fixed clock period τ, by choosing N to be the integer closest to T/τ. Finally, values of N may be computed offline and stored, yielding a finite-length segment of an AFRP. If this segment is repeated periodically, then the resulting power spectrum will be approximately $1/f^D$ for frequencies much greater than the repeat frequency of the sequence, and much smaller than the clock frequency.

E. Ionic currents in cell membranes

Ion channels are openings in the membranes of cells which allow ions to diffuse into or out of a cell [44]. These channels are usually specific to a particular ion or group of related ions, and block the passage of other species of

ions. Further, most channels have gates, and thus the channels may be either open or closed. In most cases intermediate conduction states are not observed. A few ion channels may be modeled by a two-state Markov process, with one state representing the open channel, and the other representing the closed channel. This model generates exponentially distributed dwell times in both states. However, many ion channels exhibit power-law distributed closed times and relatively short, exponentially distributed open times [45], and are well described by a marked version of the SFRP. The relatively short open times are modeled by Dirac δ functions, which suffices for all but the highest-frequency scales. The AFRP model, in contrast, describes the activity of other ion channels for which the open and closed times are similar and fractal. Whole cell ion currents exhibit spontaneous fluctuations due to the additive effects of large numbers of ion channels on the cell membrane. If these ion channels are independent of each other, then this model predicts that the whole cell ion current will be Gaussian-distributed $1/f^D$ noise. Even for dependent ion channels, evidence exists that the overall effect will be the same, although with a higher variance than for the independent channel case [46]. Indeed, the spontaneous voltage fluctuations of neurons often exhibit Gaussian-distributed $1/f^D$ noise [47].

VII. CONCLUSION

We have developed two fractal renewal processes, the SFRP and the AFRP, for which the associated interevent-time probability density functions decay in a power-law fashion. We then derived a number of the statistical properties of these FRPs, including the power spectral densities, event number moments, coincidence rates, capacity dimension, and autocorrelation functions. All of these measures exhibit power-law variation, indicating that the SFRP and AFRP are fractal. Finally, we considered a number of applications, showing that FRPs are useful in understanding a wide variety of phenomena in engineering, physics, and biology. The SFRP and the AFRP are therefore useful additions to the family of fractal processes, which include fractal shot noise [15–17], fractionally integrated white noise and fractal Brownian motion [19–21], and the fractal-shot-noise-driven doubly stochastic Poisson point process [24].

ACKNOWLEDGMENTS

This work was supported by the Joint Services Electronics Program through the Columbia Radiation Laboratory and by the Office of Naval Research under Grant No. N00014-92-J-1251.

[1] A. van der Ziel, Adv. Electron. and Electron Phys. **49**, 225 (1979).
[2] V. Radeka, IEEE Trans. Nucl. Sci. **NS-16**, 17 (1969).
[3] M. J. Buckingham, *Noise in Electronic Devices and Systems* (Wiley-Halsted, New York, 1983).
[4] A. van der Ziel, Proc. IEEE **76**, 233 (1988).
[5] M. B. Weissman, Rev. Mod. Phys. **60**, 537 (1988).
[6] P. H. Handel, Phys. Rev. A **3**, 2066 (1971).
[7] F. N. Hooge, Physica **83B**, 14 (1976).
[8] D. A. Bell, J. Phys. C **13**, 4425 (1980).
[9] J. B. Johnson, Phys. Rev. **26**, 71 (1925).
[10] T. Musha and H. Higuchi, Jpn. J. Appl. Phys. **15**, 1271 (1976).
[11] T. Geisel, A. Zacherl, and G. Radons, Phys. Rev. Lett. **59**, 2503 (1987).
[12] T. Musha, K. Sugita, and M. Kaneko, in *Noise in Physical Systems and 1/f Noise*, edited by M. Savelli, G. Lecoy, and J-P. Nougier (Elsevier, New York, 1983), p. 389.
[13] T. Musha, in *Proceedings of the 6th International Conference on Noise in Physical Systems, 1981* (Elsevier, New York, 1981), p. 143.
[14] T. Musha, Jpn. J. Appl. Phys. **26**, 2022 (1987).
[15] S. B. Lowen and M. C. Teich, Electron. Lett. **25**, 1072 (1989).
[16] S. B. Lowen and M. C. Teich, Phys. Rev. Lett. **63**, 1755 (1989).
[17] S. B. Lowen and M. C. Teich, IEEE Trans. Info. Theory **36**, 1302 (1990).
[18] H. Takayasu, J. Phys. Soc. Jpn. **56**, 1257 (1987).
[19] J. A. Barnes and D. W. Allan, Proc. IEEE **54**, 176 (1966).
[20] B. B. Mandelbrot and I. W. Van Ness, SIAM (Soc. Ind. Appl. Math.) Rev. **10**, 422 (1968).
[21] B. B. Mandelbrot, *The Fractal Geometry of Nature* (Freeman, New York, 1983).
[22] A. van der Ziel, Physica **16**, 359 (1950).
[23] A. L. McWhorter, in *Semiconductor Surface Physics*, edited by R. H. Kingston (University of Pennsylvania, Philadelphia, 1956).
[24] S. B. Lowen and M. C. Teich, Phys. Rev. A **43**, 4192 (1991).
[25] A. Papoulis, *Probability, Random Variables, and Stochastic Processes* (McGraw-Hill, New York, 1991).
[26] D. R. Cox and P. A. W. Lewis, *The Statistical Analysis of Series of Events* (Methuen, London, 1966).
[27] T. Lukes, Proc. Phys. Soc. London **78**, 153 (1961).
[28] S. B. Lowen, Ph.D. dissertation, Columbia University, 1992, Chap. 3.
[29] S. O. Rice (private communication with M. C. Teich, 1983).
[30] Y. Aizawa and T. Kohyama Prog. Theor. Phys. **72**, 659 (1984).
[31] W. Feller, *An Introduction to Probability Theory and its Applications* (Wiley, New York, 1971), Vol. 2.
[32] E. Çinlar, in *Stochastic Point Processes: Statistical Analysis, Theory, and Applications*, edited by P. A. W. Lewis (Wiley-Interscience, New York, 1972), p. 549.
[33] J. Orenstein, M. A. Kastner, and V. Vaninov, Philos. Mag. B **46**, 23 (1982).
[34] M. A. Kastner, in *Physical Properties of Amorphous Materials*, edited by D. Alser, B. B. Schwartz, and M. C. Steele (Plenum, New York, 1985), p. 381.
[35] T. Tiedje and A. Rose, Solid State Commun. **37**, 49 (1980).
[36] S. B. Lowen and M. C. Teich, Phys. Rev. B **46**, 1816

(1992).
[37] V. K. Bhatnagar and K. L. Bhatia, J. Non-Cryst. Solids **119**, 214 (1990).
[38] W. Tomaszewicz, Philos. Mag. Lett. **61**, 237 (1990).
[39] C. Kittel, *Introduction to Solid State Physics* (Wiley, New York, 1986).
[40] T. M. Nieuwenhuizen and M. H. Ernst, Phys. Rev. B **33**, 2824 (1986).
[41] B. B. Mandelbrot, IEEE Trans. Commun. Technol. **13**, 71 (1965).
[42] F. T. Arecchi and A. Califano, Europhys. Lett. **3**, 5 (1987).
[43] Y. Aizawa and T. Kohyama, Prog. Theor. Phys. **71**, 847 (1984).
[44] B. Sakmann and E. Neher, *Single-Channel Recording* (Plenum, New York, 1983).
[45] L. S. Liebovitch and T. I. Tóth, Ann. Biomed. Eng. **18**, 177 (1990).
[46] L. S. Liebovitch and J. Fischbarg, J. Theor. Biol. **119**, 287 (1986).
[47] A. A. Verveen and H. E. Derksen, Proc. IEEE **56**, 906 (1968).